

Article

Study on Characteristic Strength and Constitutive Model of Red Sandstone under Hydraulic Coupling

Xinwei Li ¹, Zhishu Yao ^{1,*}, Xianwen Huang ^{1,2}, Xiaohu Liu ¹ and Xuesong Wang ¹

¹ School of Civil Engineering and Architecture, Anhui University of Science and Technology, Huainan 232001, China

² School of Civil Engineering, Suzhou University of Science and Technology, Suzhou 215009, China

* Correspondence: zsyao@aust.edu.cn

Abstract: The newly built shaft in the western region needs to pass through the deep Cretaceous stratum, where the pores and fissures are developed, the cementation ability is poor, and the surrounding rock is rich in water. Under the coupling effect of the stress field and seepage field, the surrounding rock is easy to deteriorate and loses stability. The hydraulic coupling test of Cretaceous red sandstone was carried out by using the TAW-2000 rock mechanics testing system, and the characteristic strength evolution law of red sandstone was analyzed; Mohr's circle and strength envelope were obtained by the M–C criterion, and the influence mechanism seepage pressure on red sandstone was explored; and combined with the effective stress principle and M–C strength criterion, a constitutive model under hydraulic coupling was established. Confining pressure limits the development of cracks and strengthens the mechanical properties. The results revealed that red sandstone has the characteristics of low less clay, loose particles, and weak cementation capacity; under the action of water pressure, the cement between particles disintegrates and loses the cementation strength, resulting in a significant decrease in cohesion, and the loss of cementation strength is the internal reason for the softening of red sandstone. The constitutive model based on the effective principle and M–C criterion can better reflect the mechanical behavior of red sandstone under hydraulic coupling. This paper provides a research basis for understanding the microscopic characteristics and hydraulic coupling characteristics of Cretaceous weakly cemented sandstone.



Citation: Li, X.; Yao, Z.; Huang, X.; Liu, X.; Wang, X. Study on Characteristic Strength and Constitutive Model of Red Sandstone under Hydraulic Coupling. *Appl. Sci.* **2023**, *13*, 391. <https://doi.org/10.3390/app13010391>

Academic Editor: Bernhard Schrefler

Received: 21 November 2022

Revised: 24 December 2022

Accepted: 25 December 2022

Published: 28 December 2022



Copyright: © 2022 by the authors. Licensee MDPI, Basel, Switzerland. This article is an open access article distributed under the terms and conditions of the Creative Commons Attribution (CC BY) license (<https://creativecommons.org/licenses/by/4.0/>).

Keywords: Cretaceous red sandstone; hydraulic coupling; M–C strength criterion; constitutive model

1. Introduction

The western region is the main battlefield of coal resources development; at present, the newly built shaft in the western region needs to pass through the Cretaceous–Jurassic strata, characterized by deep water level, many pores and fissures, poor cohesion between particles, low clay content, low strength, and easy argillation. Under the coupling effect of crustal stress and seepage pressure, the superposition of stress field and seepage field induces deterioration and instability of the surrounding rock [1–3]; therefore, it is very meaningful to study the mechanical properties and failure mechanism of Cretaceous Jurassic strata under high geostress and high seepage pressure to evaluate the security of the surrounding rock and prevent water inrush and other disasters [4–9].

Water has a softening effect on the rock [10–13]. Wang et al. [14] carried out a triaxial seepage test and found the evolution law of peak strength and elastic modulus of red sandstone with confining pressure and seepage pressure. Ma et al. [15] found that water erosion occurred in the seepage process of red sandstone, and small particles migrated inside the sample, leading to the increase in porosity and attenuation of mechanical characteristics. Liu et al. [16] found that under the action of hydraulic confining pressure for a long time, water enters the rock through cracks or fractures and exerts a splitting effect on the crack, thus promoting the crack expansion. Kou et al. [17] found that the internal

pore water pressure has effects on the final failure mode. Li et al. [18] studied the failure characteristics of sandstone and explored the crack initiation and fracture mechanism under hydraulic-mechanical coupling. Chen et al. [19] found that the failure mode of sandstone under the action of seepage pressure became complex. Liu et al. [20] found that the shear cracks of a rock formed during the failure process will increase under water pressure. Essayad et al. [21] conducted the consolidation test of hard rock tailings under the action of pore water pressure, and obtained the influence of pore water pressure on the compression parameters. Pirhooshyaran et al. [22] simulated the coupling effect of hydraulic fracture and primary fracture, which was verified by the Brazil test. In the process of loading, the damage accumulates continuously and finally leads to failure [23–26]. In terms of a constitutive model, many scholars combine damage mechanics with statistics to form a mesostatistical damage theory. Hajiabadi et al. [27], based on shear failure and creep, proposed a constitutive model that can reflect the loading rate of chalk. For a high-porosity rock, Richards et al. [28] proposed a constitutive model considering hydrostatic unloading response and plastic volumetric strain. Tomac et al. [29,30] established a hydraulic fracturing model considering the strain rate and pore water pressure. Wang et al. [31] considered the process of degradation; a constitutive model under hydrological conditions was established. Bian et al. [32] considered the influence of the compression stage; a damage constitutive model considered a weak water effect was established. Song et al. [33], combined with the composite power function, established the constitutive model reflecting the osmotic pressure. Liu et al. [34] used strain as a damage factor to describe the damage caused by crack generation and propagation; a stress seepage damage constitutive model was established, but it could not reflect the impact of seepage pressure on damage.

Therefore, in this paper, the Cretaceous weakly cemented red sandstone was taken as the research object, and the hydraulic coupling test was conducted to analyze the influence of different seepage pressures on the hydraulic properties; considering the influence of seepage pressure and combined with a generalized effective stress principle, strain equivalence theory and M–C criterion introduced the damage threshold, and a hydraulic coupling damage constitutive mode was established. Compared with previous studies, this paper systematically studied the mechanical characteristics and seepage characteristics of Cretaceous weakly cemented sandstone and carried out a quantitative analysis; the constitutive model can reflect the contribution of load and osmotic pressure to damage, with clear physical meaning and closer to the actual situation.

2. Engineering Background and Microcharacteristics of Red Sandstone

2.1. Engineering Background

The Kekegai Coal Mine is located in Yulin City, Shaanxi Province, with a design production capacity of 10 Mt/a. The central air inlet and return shaft is the first shaft constructed by the drilling method in China's western region. According to the exploration data of the shaft inspection hole, the central air return shaft passes through the strata from top to bottom, which are the Quaternary, Cretaceous, and Jurassic strata. The red sandstone was taken from the Cretaceous strata.

2.2. Microcharacteristics

The composition analysis test of red sandstone was conducted by EDS, as shown in Figure 1; the sample mainly includes O, Si, Pt, C, Al, Mg, Fe, Ca, K, Na, and Ti. The content of the O element is the most abundant, followed by the Si element.

Figure 2 shows the morphological characteristics of the fracture. Mineral particles are bonded together through cement. The uncoordinated deformation of particles leads to stress concentration; therefore, the particle cross section on the fracture surface presents an irregular orientation in the microview. In the process of deformation, the clay cementitious material is destroyed, the cracks generated will continuously open and close, and the friction between local particles will make the microstructure stagger, causing changes in macromechanical properties of weakly cemented rocks. The cementation material is

between particles, the skeleton structure is loose, and the degree of compaction is low. The cementation material contains many micropores. After the destruction of the cementation material, the micropores are exposed, resulting in the discrete distribution of concave convex cavities on the failure surface, and there are a large number of loose particles on the fracture surface.

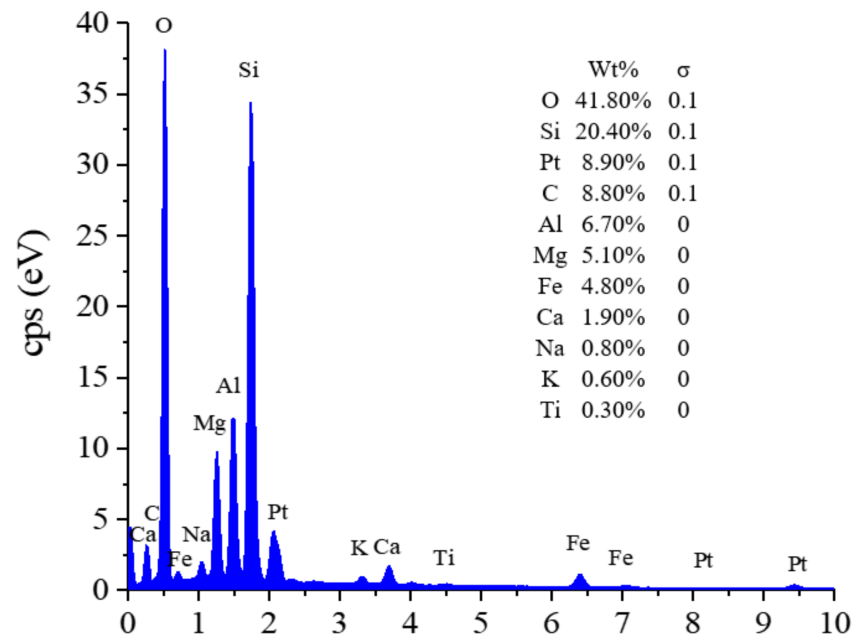


Figure 1. EDS energy spectrum.

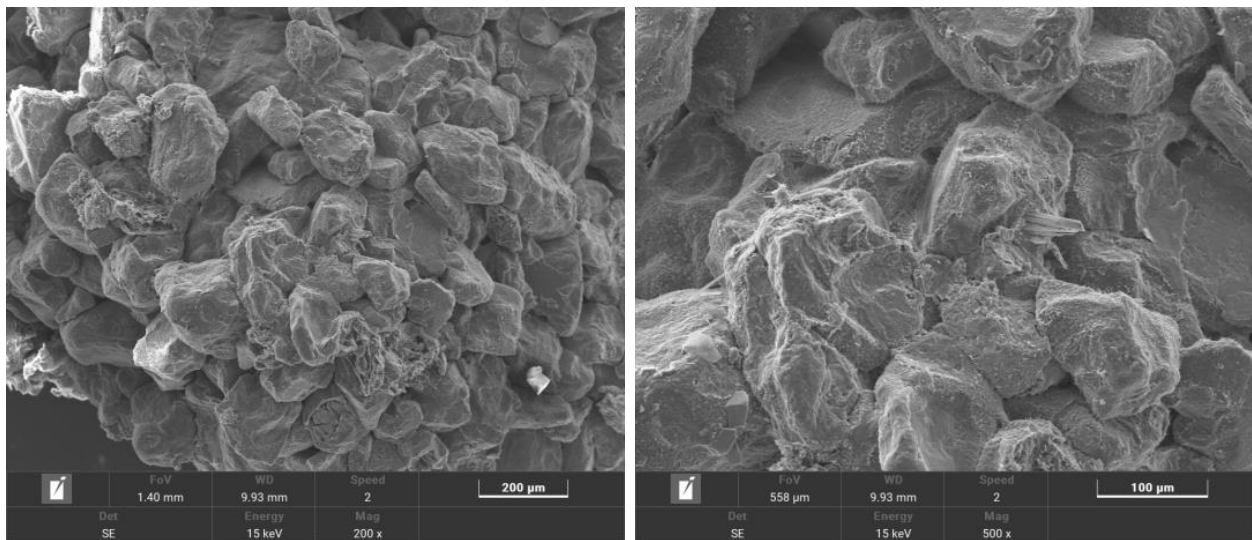


Figure 2. Microcosmic appearance.

Figure 3 shows the intensity of the diffraction peak obtained by testing with an X-ray diffractometer. Mineral matching is carried out through the built-in database to obtain the mineral composition and content of the rock, as shown in Figure 4. The basic skeleton structure of red sandstone is composed of minerals such as orthoclase, quartz, plagioclase, and calcite. The minerals that play the role of cementation are mainly clay minerals, such as montmorillonite, chlorite, illite, and kaolinite. Among them, skeleton particles account for 86.8%, cement accounts for 13.2%, and cement accounts for a small proportion.

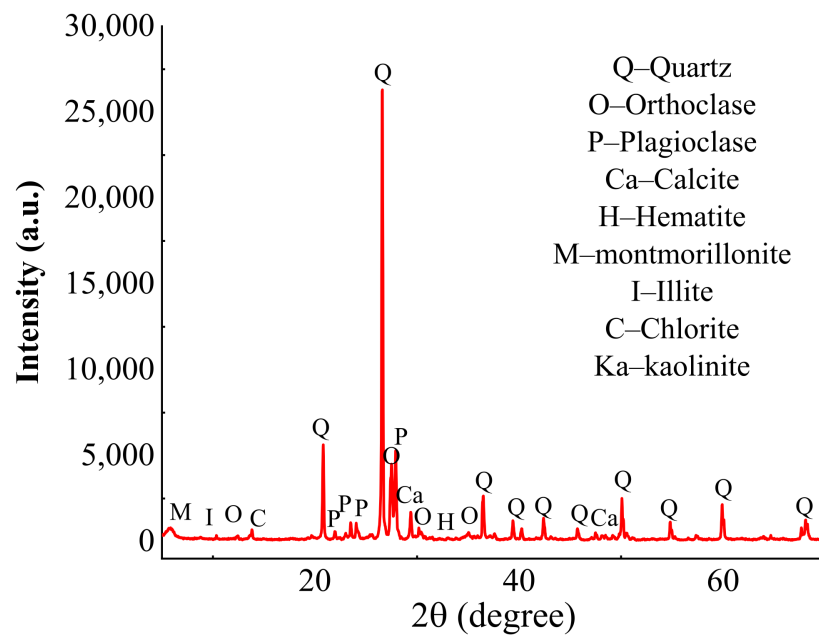


Figure 3. XRD diffraction patterns.

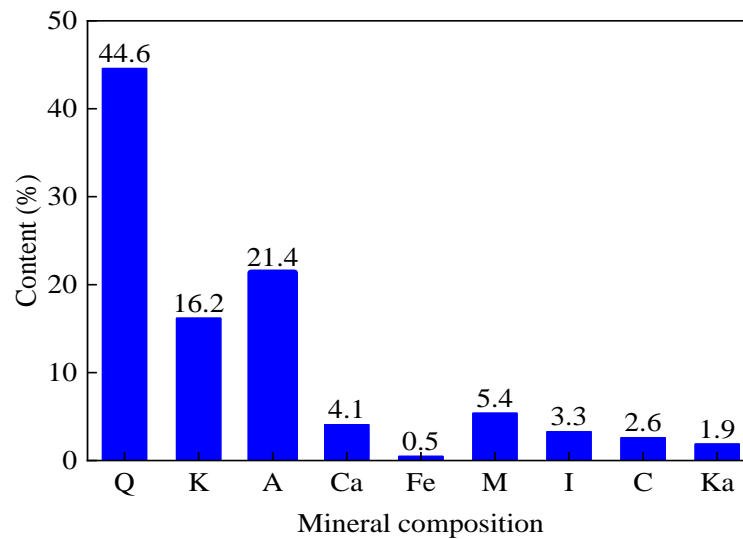


Figure 4. Mineral composition diagram.

Mineral composition and microstructure essentially affect the macromechanical properties of red sandstone. Most clay minerals are hydrophilic. During the water–rock interaction, the cement absorbs water, expands, and disintegrates. The skeleton structure bonded by the cement tends to be loose, indicating that the content of clay minerals is low and the stability is poor, which is the direct reason for the weak cementation ability of Cretaceous red sandstone.

3. Hydraulic Coupling Test

3.1. Test Instrument

Figure 5 shows the test equipment and rock samples, the TAW-2000 rock mechanics testing system, and it can realize the hydraulic-mechanical coupling test. The size of the rock sample used in the test is 50 mm × 100 mm; the wave velocity test shall be carried out before the experiment to eliminate uneven samples.

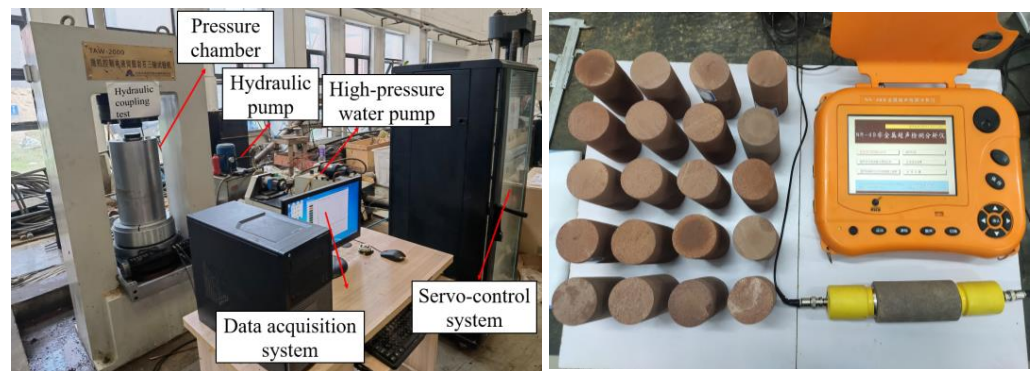


Figure 5. TAW-2000 rock mechanics testing system and rock samples.

3.2. Test Scheme

To compare the influence of seepage pressure on the results, the test was divided into two groups. The first group carried out a conventional triaxial test; that is, the seepage pressure was 0 MPa, and the confining pressures were 0, 4, 6, 8, and 10 MPa.

The second group conducted a hydraulic-mechanical coupling test. Figure 6 shows a schematic diagram of the hydraulic-mechanical coupling test. Before the test, the prepared sample is saturated with water in a vacuum for 24 h through a vacuum saturation instrument. After water saturation, hydraulic coupling tests are carried out for Cretaceous red sandstone. The confining pressures are 4, 6, 8, and 10 MPa, and the water pressures are 1, 2, and 3 MPa.

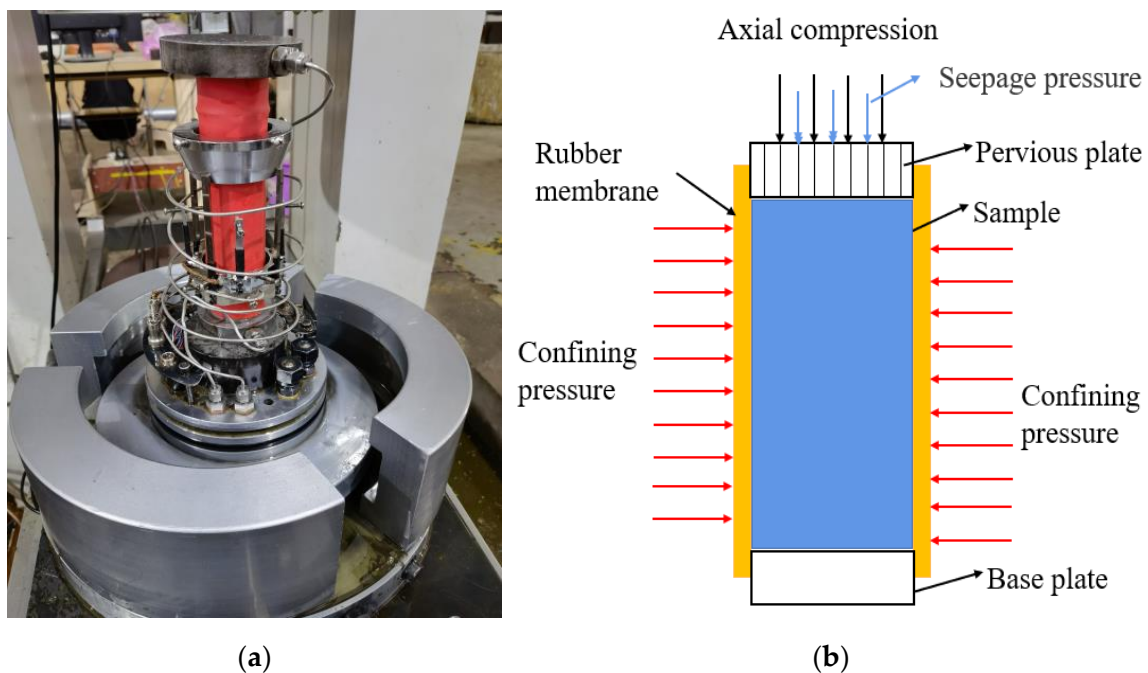


Figure 6. Schematic diagram of the hydraulic-mechanical coupling test: (a) installation drawing of sample, (b) schematic of pressure.

During the test, ensure that the confining pressure is greater than the seepage pressure, and use the rubber film and heat shrink tube to seal the sample. First, apply an axial force of about 0.5 kN to fix the sample, and then apply the confining pressure. After the confining pressure reaches the preset value and becomes stable, apply the seepage pressure. After the seepage pressure reaches the preset values and becomes stable, the axial force is applied through deformation control until failure, and the loading speed is 0.01 mm/min.

4. Test Results and Analysis

4.1. Stress–Strain Curve

In this paper, conventional triaxial tests and triaxial hydraulic coupling tests were carried out. Figure 7 shows that confining pressure and seepage pressure can significantly affect the strength and deformation characteristics; with the increase in confining pressure, the strength increases, and the resistance to deformation increases. The effect of osmotic pressure is opposite.

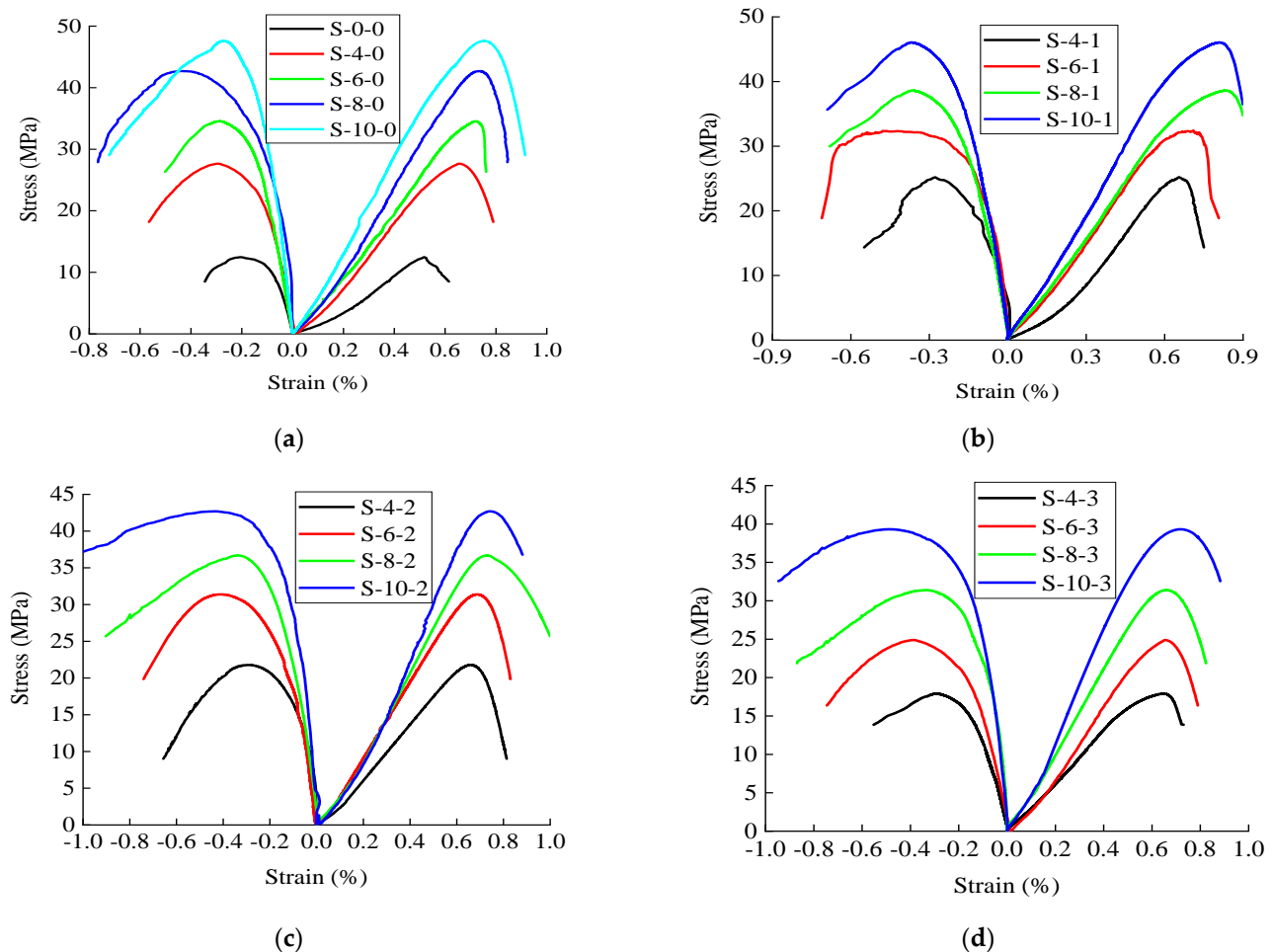


Figure 7. Stress–strain curves: (a) seepage pressure is 0 MPa, (b) seepage pressure is 1 MPa, (c) seepage pressure is 2 MPa, and (d) seepage pressure is 3 MPa.

4.2. Crack Volume Model

The crack volume model was the primary method for determining the crack initiation and penetration of rocks [35,36]. Figure 8 shows a schematic diagram of phase division and characteristic strength; this method is to determine the crack closure strength (σ_c), crack initiation strength (σ_i), dilatancy strength (σ_d), and peak strength (σ_f). The volume strain curve and volume strain curve of the crack show compression first and then expansion.

In the crack closure stage, the original microcracks and pores are closed, and the crack volume strain is gradually reduced. In the crack stable development stage, the volume strain increment is approximately equal to the elastic volume strain increment, and the crack does not expand significantly, so the crack volume strain curve is approximately horizontal. In the crack unstable development stage, the crack propagation and the crack volume strain curve deflect to the negative direction. In the dilatancy stage, the rock transforms from volume compression to volume expansion; the volume strain expansion rate of the crack

is relatively large, and the rock enters an obvious yield state. In the postpeak stage, the internal fracture surface of the rock expands and penetrates, and the rock failure.

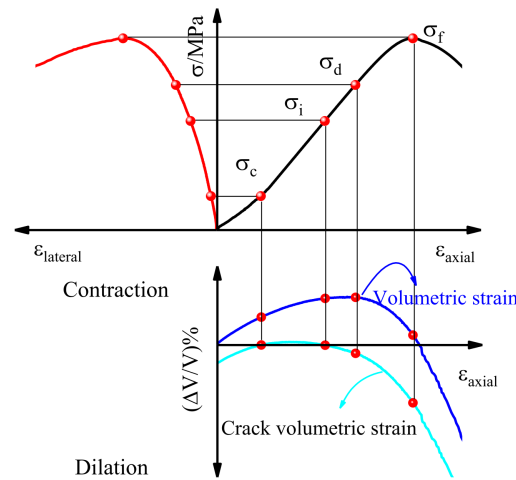


Figure 8. Schematic diagram of phase division and characteristic stress.

The volume strain, volume crack strain, and volume elastic strain meet the following relations:

$$\epsilon_{vc} = \epsilon_v - \epsilon_{ve} \tag{1}$$

During the rock compression test, the volume strain ϵ_v was expressed as

$$\epsilon_v = \epsilon_1 + \epsilon_2 + \epsilon_3 \tag{2}$$

Assuming that the volume increment is composed of elastic strain and crack increment strain, the elastic volume strain considering seepage pressure can be expressed as

$$\epsilon_{ve} = \frac{(1 - 2\mu)(\sigma_1 + \sigma_2 + \sigma_3 - 3\alpha P_w)}{E} \tag{3}$$

where ϵ_v is the volume strain, ϵ_{ve} is the volume elastic strain of the rock, and ϵ_{vc} is the crack volume strain of the rock.

4.3. Evolution of Characteristic Strength

Figure 9 shows the evolution law of the characteristic strength of red sandstone. Through linear regression of the relationship curve between the strength and confining pressure of red sandstone, and it was found that each characteristic strength and confining pressure approximately meet the linear relationship.

Seepage pressure can accelerate the process of crack development and weaken the strength. With the increase in seepage pressure, the crack closure stress, crack initiation stress, dilatation stress, and peak stress of the rock are reduced. Confining pressure delays the process of failure and limits the formation of cracks. Confining pressure suppresses the effect of seepage pressure; the greater the confining pressure is, the weakening effect of seepage pressure on the strength decreases. This is because under the effect of seepage pressure, pore and fissure water produce expansion tension on the pore and fissure tip, which accelerates the expansion of pore and fissure.

With the increase in seepage pressure, the strength growth rate of red sandstone under unit confining pressure increases. Taking the peak stress of red sandstone as an example, when the water pressure is 0, 1, 2, and 3 MPa, the strength growth rates under the unit confining pressure are 3.3, 3.45, 3.51, and 3.61, respectively, indicating that the greater the seepage pressure is, the better the strengthening effect of confining pressure on strength is.

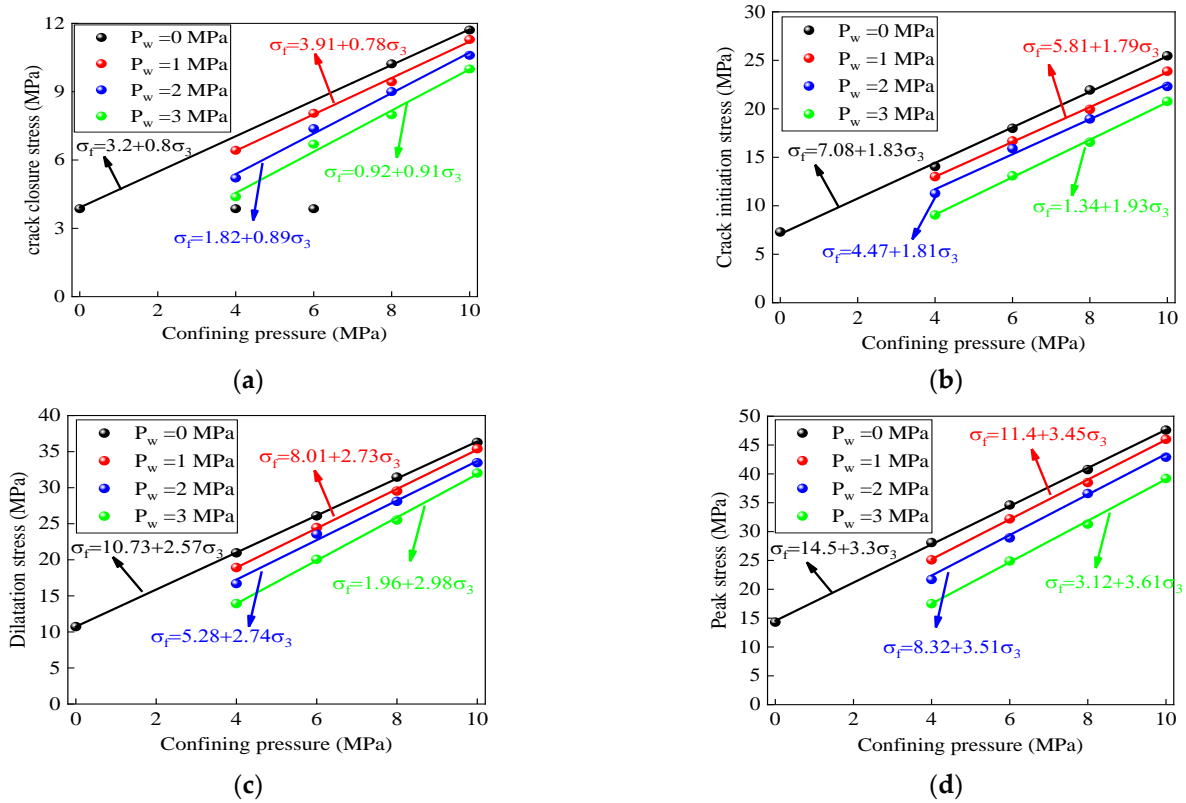


Figure 9. Variation curve of characteristic strength: (a) crack closure strength, (b) crack initiation stress, (c) dilatation strength, and (d) peak strength.

4.4. Deterioration Mechanism Caused by Water Pressure

Mohr’s circles and stress envelopes were obtained by the M–C strength criterion. The cohesion and internal friction angle are calculated according to the following formula:

$$c = \frac{b}{2\sqrt{k}}, \varphi = \arcsin\left(\frac{k-1}{k+1}\right) \quad (4)$$

where k and b are the slope and intercept of the peak strength—confining pressure curve in Figure 9d.

As shown in Figure 10, under the effect of 0–3 MPa seepage pressure, the internal friction angle of red sandstone is between 32.3° and 34.5° , and the cohesion is between 0.8 and 4 MPa. With the increase in seepage pressure, the internal friction angle increases slowly, indicating that water pressure has a reduction on the internal friction angle of weakly cemented sandstone. The seepage pressure will affect the cohesion, which decreases with the increase in seepage pressure; when the seepage pressure increases to 3 MPa, the cohesion is only 20% of that without seepage pressure. This is because Cretaceous red sandstone has the characteristics of poor cementation capacity; under the effect of seepage pressure, the particles are dissolved, and the cements between particles lose their cementation strength, so the cementation is weakened. Moreover, in the loading process, the seepage pressure will inevitably produce expansion tension on the tip of the pore fracture, further reducing the cementation.

Mineral composition and microstructure essentially affect the macromechanical properties of red sandstone. Most clay minerals are hydrophilic. In the process of water–rock interaction, the cement absorbs water, expands, and disintegrates. The skeleton structure bonded by the cement tends to be loose, indicating that the low content of clay minerals is the direct reason for the weak cementation ability of Cretaceous red sandstone. Under the action of hydraulic coupling, seepage pressure accelerates the dissolution of cemen-

titious materials, increases the scouring of pores and fissures, and causes the decrease in internal cohesion and loosening of particles. The seepage volume force increases the expansion of pores and fissures and the scouring of particles increases, which speeds up the disintegration of the internal structure of sandstone.

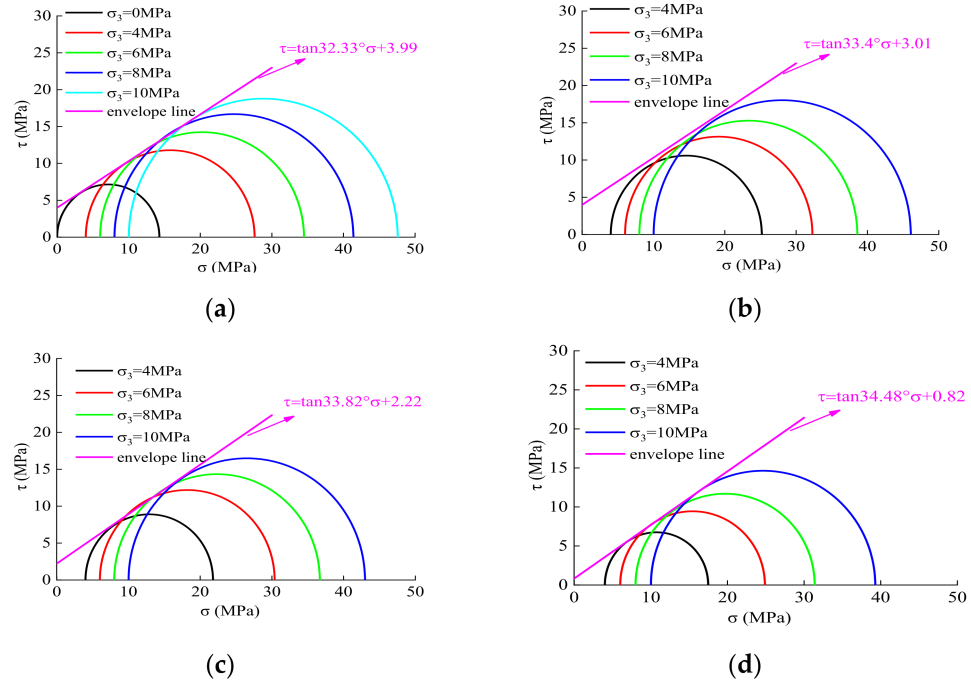


Figure 10. Mohr’s circle and envelope line under different confining pressures and seepage pressures: (a) seepage pressure is 0 MPa, (b) seepage pressure is 1 MPa, (c) seepage pressure is 2 MPa; (d) Seepage pressure is 3 MPa.

5. Damage Constitutive Model Considering Seepage Pressure

5.1. Effective Stress Principle

The applicable constitutive model is very important for simulating the stress–strain relationship of materials [37]. The statistical damage constitutive model has the characteristics of clear parameter meaning and wider applicability. Therefore, this paper selects the statistical damage constitutive model to simulate the stress–strain curve of the rock. In this paper, the hydraulic coupling effect is considered, and the connection between stress and seepage pressure is established through the principle of effective stress [38,39]:

$$\sigma'_{ij} = \sigma_{ij} - \alpha P_w \delta_{ij} \tag{5}$$

where σ'_{ij} is the effective stress tensor, σ_{ij} is the total stress tensor, α is the effective stress coefficient, P_w is the seepage pressure, and δ_{ij} is the second-order tensor.

5.2. Construction of the Constitutive Model

According to the hypothesis of equivalent strain [40–42],

$$\tilde{\sigma}_{ij} = \frac{\sigma_{ij}}{1 - D} \tag{6}$$

By combining Formulas (5) and (6), it can be obtained that the damage constitutive relationship of porous elastic materials under hydraulic coupling is

$$\tilde{\sigma}'_{ij} = \frac{\sigma'_{ij}}{1 - D} = \frac{\sigma_{ij} - \alpha P_w \delta_{ij}}{1 - D} \tag{7}$$

Assume that a large number of microelements constitute the rock, and the microelement strength is randomly distributed; therefore, the probability density of the Weibull distribution [43] is

$$P(f_{(\sigma)}) = \frac{m}{k} \left(\frac{f_{(\sigma)}}{k}\right)^{m-1} \exp\left[-\left(\frac{f_{(\sigma)}}{k}\right)^m\right] \tag{8}$$

where k and m are parameters of the model, and $f_{(\sigma)}$ is the rock yield criterion.

Therefore, the damage variable D [44] can be expressed as

$$D = 1 - \exp\left[-\left(\frac{f_{(\sigma)}}{F_0}\right)^m\right] \tag{9}$$

The value range of D is (0~1), $D = 0$ represents the initial state or no damage state, and $D = 1$ represents the complete damage state.

The microelement strength function is established based on the strength criterion. The rock microelement strength described by the M-C strength criterion [45,46] is

$$f_{(\sigma)} = \sigma_1 - \sigma_3 \frac{1 + \sin \varphi}{1 - \sin \varphi} - \frac{2c \cos \varphi}{1 - \sin \varphi} \tag{10}$$

The traditional M-C criterion is insufficient to describe the rock stress state under hydraulic coupling; therefore, the seepage pressure is introduced. In combination with Formulas (5) and (10), an improved M-C criterion reflecting the effect of hydraulic coupling is obtained:

$$f_{(\sigma')} = \sigma'_1 - \sigma'_3 \frac{1 + \sin \varphi}{1 - \sin \varphi} + \frac{2\alpha \sin \varphi}{1 - \sin \varphi} P_w - \frac{2c \cos \varphi}{1 - \sin \varphi} \tag{11}$$

Combining Equations (7) and (11), the microelement strength function based on the improved M-C criterion was obtained:

$$f_{(\sigma)} = \frac{((1 - \sin \varphi)\sigma_1 - (1 + \sin \varphi)\sigma_3 + 2\alpha \sin \varphi P_w)E\varepsilon_1}{(1 - \sin \varphi)(\sigma_1 - 2\mu\sigma_3 - (1 - 2\mu)\alpha P_w)} - \frac{2c \cos \varphi}{1 - \sin \varphi} \tag{12}$$

where $\frac{2c \cos \varphi}{1 - \sin \varphi}$ is the damage threshold, which means that when $f_{(\sigma)} \geq 0$, the rock enters the yield stage and the damage starts to appear.

It can be seen that the existence of seepage pressure accelerates the process of sandstone's failure. Axial stress and seepage pressure play a positive role in rock yield, while confining pressure plays a restraining role in rock yield.

Hooke's law is expressed as

$$\tilde{\varepsilon}'_1 = \frac{1}{E} [\tilde{\sigma}'_1 - \mu(\tilde{\sigma}'_2 + \tilde{\sigma}'_3)] \tag{13}$$

By substituting Equations (6) and (12) into Equation (13), the rock hydraulic coupling damage constitutive model is obtained:

$$\sigma_1 = E\varepsilon_1 \exp\left[-\left(\frac{f_{(\sigma)}}{k}\right)^m\right] + 2\mu\sigma_3 + (1 - 2\mu)\alpha P_w \tag{14}$$

This is the general form of the hydraulic coupling damage constitutive model, which can degenerate into the classical linear elastic constitutive model in the nondamage state; whether there is damage is determined according to Equation (12). When seepage water pressure is not considered, it can be reduced to the constitutive model based on the M-C criterion [47].

5.3. Solution of Model Parameters

The model’s parameters play a key role in establishing a statistical damage constitutive model. Usually, many methods are used to determine parameters [48]. The curve fitting method was adopted in this paper.

Equation (14) was transformed and put forward the exponential term:

$$\exp \left[- \left(\frac{f(\sigma)}{k} \right)^m \right] = \frac{\sigma_1 - 2\mu\sigma_3 - (1 - 2\mu)\alpha P_w}{E\varepsilon_1} \tag{15}$$

The values of m and k can be obtained by linear regression. Thus, the hydraulic coupling damage constitutive model considering the improved M–C criterion can be determined. By taking logarithms twice to Equation (15), Equation (16) is obtained:

$$y = mx - b \tag{16}$$

where

$$y = \ln \frac{E\varepsilon_1}{\sigma_1 - 2\mu\sigma_3 - (1 - 2\mu)\alpha P_w} \tag{17}$$

$$x = \ln f(\sigma) \tag{18}$$

$$b = -m \ln k \tag{19}$$

5.4. Model Validation

The constitutive model is verified by triaxial hydraulic coupling test results of Cretaceous red sandstone; the relevant model parameters are shown in Table 1. As shown in Figure 11, the theoretical curve basically coincides with the test curve; this model can accurately capture the nonlinearity near the peak. This shows that the damage constitutive model can reflect the strength characteristics and stress–strain relationship of red sandstone under hydraulic coupling, and verifies the rationality and applicability of the hydraulic coupling damage constitutive model. To some extent, it can predict the mechanical behavior of red sandstone under a complex stress state.

Table 1. Parameters of statistical damage model.

Number	Seepage Pressure (MPa)	Cohesion (MPa)	Internal Friction Angle (°)	Confining Pressure (MPa)	Peak Strength (MPa)	Peak Strain	Elastic Modulus (MPa)	Poisson’s Ratio	m	k
S-0-0	0 MPa	3.99	32.33	0	14.5	0.00519	3800	0.325	8.8	11.3
S-4-0				0	27.9	0.00658	5350	0.292	9.5	26.7
S-6-0				0	31.5	0.00725	5600	0.271	10.2	32.5
S-8-0				0	41.4	0.00737	7300	0.257	11.3	40.4
S-10-0				0	47.6	0.00759	7600	0.236	12.6	44.5
S-4-1	1 MPa	3.01	33.4	1	25.2	0.00655	4800	0.302	14.3	22.5
S-6-1				1	32.4	0.00713	5500	0.281	14.7	30.1
S-8-1				1	38.6	0.00832	5700	0.266	15.1	35.3
S-10-1				1	46.1	0.00810	6600	0.245	16.3	41.5
S-4-2	2 MPa	2.22	33.82	2	21.8	0.00658	3850	0.311	12.5	20.8
S-6-2				2	30.4	0.00687	5100	0.298	13.8	27.2
S-8-2				2	36.7	0.00729	6500	0.276	14.6	32.5
S-10-2				2	43.1	0.00743	7200	0.256	15.4	43.1
S-4-3	3 MPa	0.82	34.48	3	17.5	0.00649	3400	0.314	11.6	18.6
S-6-3				3	24.9	0.00655	4600	0.295	12.5	26.7
S-8-3				3	31.4	0.00673	5700	0.276	13.9	33.4

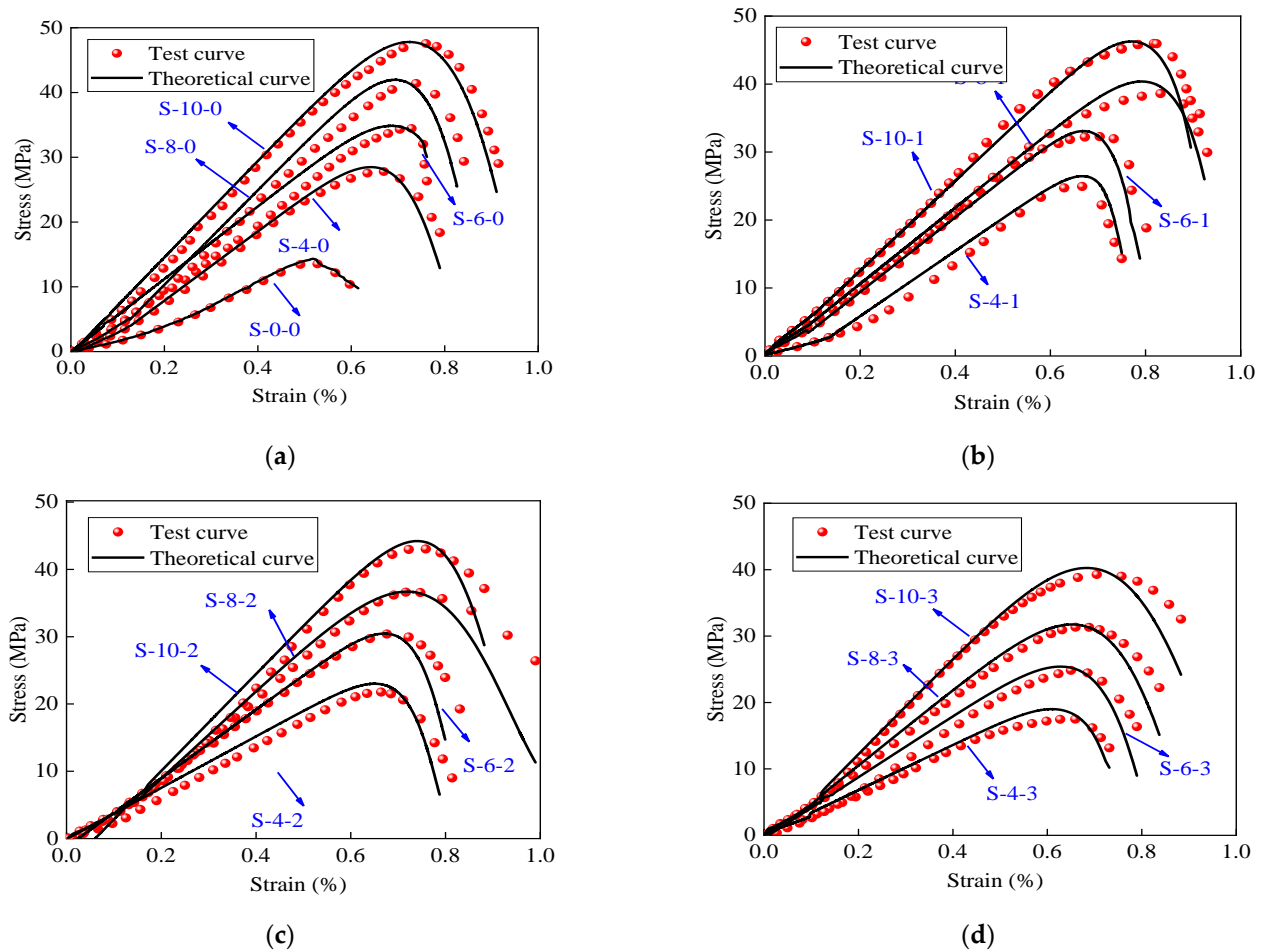


Figure 11. Comparison between experimental curve and theoretical curve. (a) Seepage pressure is 0 MPa, (b) seepage pressure is 1 MPa, (c) seepage pressure is 2 MPa, and (d) seepage pressure is 3 MPa.

5.5. Parameter Sensitivity Analysis

Sensitivity analysis is an indispensable link in numerical simulation research [49,50]. Because it can screen out the key parameters that affect the effectiveness of the model, it is of great significance in the quantification of model uncertainty and parameter calibration. Through sensitivity analysis, this paper mainly discusses the physical meaning represented by the parameter and the influence of the parameter on the shape. The high and low of sensitivity or the sensitivity index is not the focus of this paper; moreover, the model parameters are only m and k , so this paper only carries out local sensitivity analysis.

To explain the physical significance of parameters, the stress–strain curve sample of S-4-2 is selected for the sensitivity analysis of the parameters m and k . Keep the value of k unchanged; take m as 5, 10, 15, and 20; and then draw the stress–strain curve. As shown in Figure 12, the change of parameter m produces an effect on the shape of the stress–strain curve. With the increase in m , the peak strength and peak strain increase, the increase in peak intensity gradually decreases, the postpeak curve becomes steep, and the stress–strain curve changes from strain softening to strain hardening, indicating that the parameter m reflects the plastic deformation characteristics.

Keep the value of m unchanged; take k as 10, 15, 20, and 25; and then draw the stress–strain curve. As shown in Figure 13, the peak strength increases with the increase in k ; the strength of the rock increases, indicating that the rock's resistance to failure and deformation is enhanced; the brittleness is enhanced; and the failure becomes sudden. It shows that k affects the strength and brittleness of the rock.

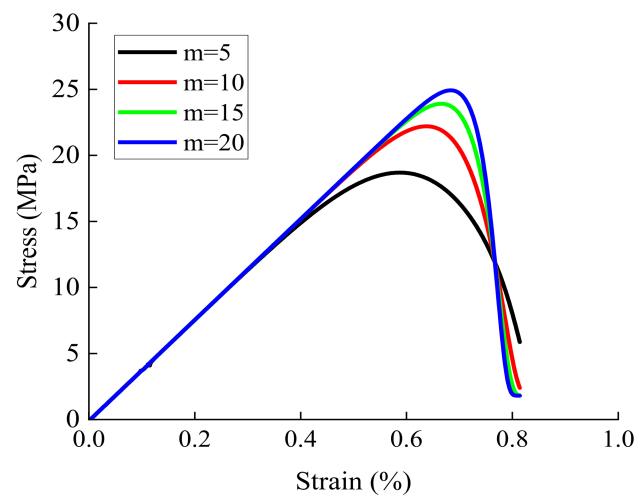


Figure 12. Sensitivity analysis of parameter m .

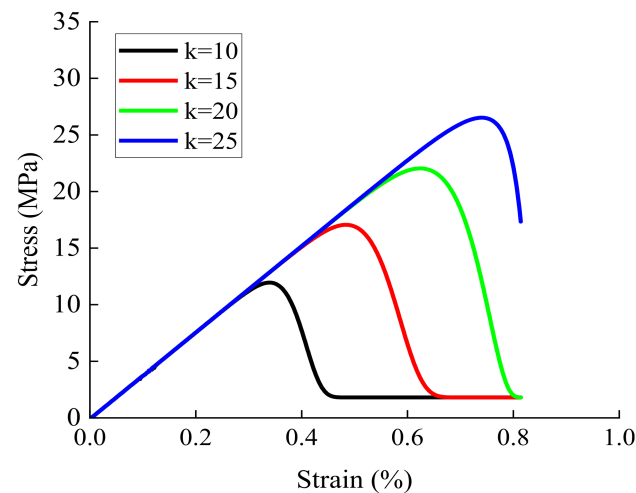


Figure 13. Sensitivity analysis of parameter k .

6. Conclusions

A series of tests, such as a scanning electron microscope and a hydraulic coupling test, were carried out to analyze the micro- and macromechanical characteristics of weakly cemented red sandstone, and a hydraulic coupling constitutive model was derived. The following conclusions were obtained through experiments and theoretical studies:

- (1) The evolution laws of characteristic strength of red sandstone are obtained by the volume strain method. Confining pressure limits crack propagation and enhances strength. With the increase in confining pressure, crack closure strength, crack initiation strength, dilatancy strength, and peak strength increase. The seepage pressure accelerates the crack propagation and weakens the strength, and the effect of seepage pressure is opposite to that of confining pressure.
- (2) Cretaceous red sandstone has few clay minerals, loose structure, low cohesion, and weak cementation ability. Under the action of seepage pressure, the cement between particles is dissolved, and the cement strength is easily lost. In addition, the water pressure produces expansion tension on the tip of pores and fractures, speeding up the expansion of pores and fractures, resulting in a significant decrease in cohesion, which shows an obvious softening effect.
- (3) The seepage pressure action term is introduced into the M–C criterion, and the element strength function that can reflect the influence of seepage pressure is obtained by combining the effective stress principle and strain equivalence theory.

- (4) The model can better reflect the stress–strain relationship of red sandstone under the hydraulic coupling action, and has wide application. At the same time, it can degenerate into a conventional damage constitutive model without the action of seepage pressure.

Author Contributions: Conceptualization, X.L. (Xinwei Li) and X.H.; methodology, Z.Y.; investigation, X.H.; data curation, X.L. (Xiaohu Liu) and X.W.; writing—original draft preparation, X.L. (Xinwei Li); writing—review and editing, X.H.; project administration, X.W.; funding acquisition, Z.Y. All authors have read and agreed to the published version of the manuscript.

Funding: This research was funded by the graduate research project of Anhui Provincial Department of Education (YJS20210382), China Scholarship Council (202108340062), Anhui Provincial College of Natural Science Research Key Project (KJ2018A0098), China Postdoctoral Science Foundation (2018M642502), Jiangxi Geological Environment and Underground Space Engineering Research Center (JXDHJJ2021-008), State Key Laboratory of Nuclear Resources and Environment (2022NRE07), and Engineering Research Center of the Ministry of Education of Mine Underground Engineering (JYBGCZX2022105).

Institutional Review Board Statement: Not applicable.

Informed Consent Statement: Not applicable.

Data Availability Statement: Not applicable.

Conflicts of Interest: The authors declare no conflict of interest.

References

- Zhang, Q.; Shao, C.; Wang, H.; Jiang, B.; Jiang, Y.; Liu, R. A fully coupled hydraulic-mechanical solution of a circular tunnel in strain-softening rock masses. *Tunn. Undergr. Space Technol.* **2020**, *99*, 103375. [[CrossRef](#)]
- Zhao, C.; Zhang, Z.; Lei, Q. Role of hydro-mechanical coupling in excavation-induced damage propagation, fracture deformation and microseismicity evolution in naturally fractured rocks. *Eng. Geol.* **2021**, *289*, 106169. [[CrossRef](#)]
- Ma, D.; Rezaia, M.; Yu, H.; Haibo, B. Variations of hydraulic properties of granular sandstones during water inrush; effect of small particle migration. *Eng. Geol.* **2017**, *217*, 61–70. [[CrossRef](#)]
- Zhang, J.; Song, Z.; Wang, S. Mechanical behavior of deep sandstone under high stress-seepage coupling. *J. Cent. South Univ.* **2021**, *28*, 3190–3206. [[CrossRef](#)]
- Li, W.; Wang, Z.; Qiao, L.; Liu, J.; Yang, J. The effects of hydro-mechanical coupling on hydraulic properties of fractured rock mass in unidirectional and radial flow configurations. *Geomech. Geophys. Geo-Energy Geo-Resour.* **2021**, *7*, 87. [[CrossRef](#)]
- Dong, X.; Karrech, A.; Qi, C.; Elchalakani, M.; Basarir, H. Analytical solution for stress distribution around deep lined pressure tunnels under the water table. *Int. J. Rock Mech. Min. Sci.* **2019**, *123*, 104124. [[CrossRef](#)]
- Zhu, J.; Deng, J.; Chen, F.; Wang, F. Failure analysis of water-bearing rock under direct tension using acoustic emission. *Eng. Geol.* **2022**, *299*, 106541. [[CrossRef](#)]
- Liu, H.; Zhu, C.; Meng, Q.; Wang, X.; Li, X.; Wu, W. Model test on rock-socketed pile in reef limestone. *Rock Soil Mech.* **2018**, *39*, 1581–1588. (In Chinese)
- Wang, X.; Shan, H.; Wang, X.; Zhu, C. Strength characteristics of reef limestone for different cementation types. *Geotech Geol. Eng.* **2019**, *38*, 79–89. [[CrossRef](#)]
- Ma, H.F.; Song, Y.Q.; Chen, S.J.; Yin, D.W.; Zheng, J.J.; Shen, F.X.; Li, X.S.; Ma, Q. Experimental investigation on the mechanical behavior and damage evolution mechanism of water-immersed gypsum rock. *Rock Mech. Rock Eng.* **2021**, *54*, 4929–4948. [[CrossRef](#)]
- Zhu, J.; Deng, J.; Ma, Y.; Pak, R.Y.S.; Zhang, Z. Experimental study on the competing effects of strain rate and water weakening on compressive strength of saturated rocks. *Eng. Geol.* **2022**, *310*, 106873. [[CrossRef](#)]
- Earnest, E.; Boutt, D. Investigating the role of hydromechanical coupling on flow and transport in shallow fractured-rock aquifers. *Hydrogeol. J.* **2014**, *22*, 1573–1591. [[CrossRef](#)]
- Breard, E.C.P.; Dufek, J.; Fullard, L.; Carrara, A. The basal friction coefficient of granular flows with and without excess pore pressure; implications for pyroclastic density currents, water-rich debris flows, and rock and submarine avalanches. *J. Geophys. Res. Solid Earth* **2020**, *125*, e2020JB020203. [[CrossRef](#)]
- Wang, Q.; Hu, X.; Zheng, W.; Li, L.; Zhou, C.; Ying, C.; Xu, C. Mechanical properties and permeability evolution of red sandstone subjected to hydro-mechanical coupling: Experiment and discrete element modelling. *Rock Mech. Rock Eng.* **2021**, *54*, 2405–2423. [[CrossRef](#)]
- Ma, D.; Duan, H.; Li, X.; Li, Z.; Zhou, Z.; Li, T. Effects of seepage-induced erosion on nonlinear hydraulic properties of broken red sandstones. *Tunn. Undergr. Space Technol.* **2019**, *91*, 102993. [[CrossRef](#)]

16. Liu, Y.; Liu, C.; Kang, Y.; Wang, D.; Ye, D. Experimental research on creep properties of limestone under fluid–solid coupling. *Environ. Earth Sci.* **2015**, *73*, 7011–7018. [[CrossRef](#)]
17. Kou, M.; Liu, X.; Wang, Z.; Nowruzpour, M. Mechanical properties, failure behaviors and permeability evolutions of fissured rock-like materials under coupled hydro-mechanical unloading. *Eng. Fract. Mech.* **2021**, *254*, 107929. [[CrossRef](#)]
18. Li, Y.; Liu, G.; Qin, T.; Jin, Z.; Zhao, C.; Huang, S. Progressive failure and fracture mechanism of sandstone under hydraulic-mechanical coupling. *Shock Vib.* **2020**, *2020*, 8866680. [[CrossRef](#)]
19. Chen, F.; Lv, J.; Yin, Y.; Qi, C. Numerical test study on the failure mechanism of coal-rock combined body under the coupling action of hydraulic and mechanical. *Geofluids* **2022**, *2022*, 2694139. [[CrossRef](#)]
20. Liu, D.; Yan, W.; Yan, S.; Kang, Q. Study on the effect of axial and hydraulic pressure coupling on the creep behaviors of sandstone under multi-loading. *Bull. Eng. Geol. Environ.* **2021**, *80*, 6107–6120. [[CrossRef](#)]
21. Essayad, K.; Aubertin, M. Consolidation of hard rock tailings under positive and negative pore-water pressures: Testing procedures and experimental results. *Can. Geotech. J.* **2020**, *58*, 49–65. [[CrossRef](#)]
22. Pirhooshyaran, M.R.; Nikkhah, M. Hydraulic fracture patterns in fractured rock mass using coupled hydromechanical modeling in the bonded particle model. *Model. Earth Syst. Environ.* **2022**, *8*, 2277–2290. [[CrossRef](#)]
23. Zhu, C.; Zhu, P.; Liu, Z. Uncertainty analysis of mechanical properties of plain woven carbon fiber reinforced composite via stochastic constitutive modeling. *Compos. Struct.* **2019**, *207*, 684–700. [[CrossRef](#)]
24. Xiao, W.; Zhang, D.; Wang, X.; Yang, H.; Wang, X.; Wang, C. Research on microscopic fracture morphology and damage constitutive model of red sandstone under seepage pressure. *Nat. Resour. Res.* **2020**, *29*, 3335–3350. [[CrossRef](#)]
25. Zhu, Y. A micromechanics-based damage constitutive model of porous rocks. *Int. J. Rock Mech. Min. Sci.* **2017**, *91*, 1–6. [[CrossRef](#)]
26. Shariff, M.H.B.M.; Bustamante, R. A spectral approach for nonlinear transversely isotropic elastic bodies, for a new class of constitutive equation: Applications to rock mechanics. *Acta Mech.* **2020**, *231*, 4803–4818. [[CrossRef](#)]
27. Hajiabadi, M.R.; Nick, H.M. A modified strain rate dependent constitutive model for chalk and porous rock. *Int. J. Rock Mech. Min. Sci. (Oxf. Engl. 1997)* **2020**, *134*, 104406. [[CrossRef](#)]
28. Richards, M.C.; Issen, K.A.; Ingraham, M.D. A coupled elastic constitutive model for high porosity sandstone. *Int. J. Rock Mech. Min. Sci.* **2022**, *150*, 104989. [[CrossRef](#)]
29. Tomac, I.; Gutierrez, M. Micromechanics of hydraulic fracturing and damage in rock based on DEM modeling. *Granul. Matter* **2020**, *22*, 56. [[CrossRef](#)]
30. Tomac, I.; Gutierrez, M. Coupled hydro-thermo-mechanical modeling of hydraulic fracturing in quasi-brittle rocks using BPM-DEM. *J. Rock Mech. Geotech. Eng.* **2017**, *9*, 92–104. [[CrossRef](#)]
31. Wang, L.; Yin, Y.; Zhou, C.; Huang, B.; Wang, W. Damage evolution of hydraulically coupled Jianchuandong dangerous rock mass. *Landslides* **2020**, *17*, 1083–1090. [[CrossRef](#)]
32. Bian, K.; Liu, J.; Zhang, W.; Zheng, X.; Ni, S.; Liu, Z. Mechanical behavior and damage constitutive model of rock subjected to water-weakening effect and uniaxial loading. *Rock Mech. Rock Eng.* **2019**, *52*, 97–106. [[CrossRef](#)]
33. Song, Z.; Wang, T.; Wang, J.; Xiao, K.; Yang, T. Uniaxial compression mechanical properties and damage constitutive model of limestone under osmotic pressure. *Int. J. Damage Mech.* **2022**, *31*, 557–581. [[CrossRef](#)]
34. Liu, B.; Li, J.; Liu, Q.; Liu, X. Analysis of damage and permeability evolution for mudstone material under coupled stress-seepage. *Materials* **2020**, *13*, 3755. [[CrossRef](#)] [[PubMed](#)]
35. Zhao, C.; Liu, J.; Lyu, C.; Chen, W.; Li, X.; Li, Z. Experimental study on mechanical properties, permeability and energy characteristics of limestone from through-coal seam (TCS) tunnel. *Eng. Geol.* **2022**, *303*, 106673. [[CrossRef](#)]
36. Martin, C.D. Seventeenth Canadian Geotechnical Colloquium: The effect of cohesion loss and stress path on brittle rock strength. *Can. Geotech. J.* **1997**, *34*, 698–725. [[CrossRef](#)]
37. Rokhy, H.; Mostofi, T.M.; Ozbakkaloglu, T. Calibration of different constitutive material models for Vosges sandstone due to its application in rock-cutting processes. *J. Braz. Soc. Mech. Sci. Eng.* **2022**, *44*, 468. [[CrossRef](#)]
38. Chen, J.; Zhao, J.; Zhang, S.; Zhang, Y.; Yang, F.; Li, M. An experimental and analytical research on the evolution of mining cracks in deep floor rock mass. *Pure Appl. Geophys.* **2020**, *177*, 5325–5348. [[CrossRef](#)]
39. Biot, M.A. General Theory of Three-Dimensional Consolidation. *J. Appl. Phys.* **1941**, *12*, 155–164. [[CrossRef](#)]
40. Liu, Y.; Dai, F. A damage constitutive model for intermittent jointed rocks under cyclic uniaxial compression. *Int. J. Rock Mech. Min. Sci.* **2018**, *103*, 289–301. [[CrossRef](#)]
41. Zhu, H.; Zhang, Q.; Huang, B.; Zhang, L. A constitutive model based on the modified generalized three-dimensional Hoek–Brown strength criterion. *Int. J. Rock Mech. Min. Sci.* **2017**, *98*, 78–87. [[CrossRef](#)]
42. Xu, X.; Karakus, M.; Gao, F.; Zhang, Z. Thermal damage constitutive model for rock considering damage threshold and residual strength. *J. Cent. South Univ.* **2018**, *25*, 2523–2536. [[CrossRef](#)]
43. Gu, Q.; Ma, Q.; Tan, Y.; Jia, Z.; Zhao, Z.; Huang, D. Acoustic emission characteristics and damage model of cement mortar under uniaxial compression. *Constr. Build. Mater.* **2019**, *213*, 377–385. [[CrossRef](#)]
44. Lombardi, G.; Paula, A.M.; Pinho-Lopes, M. Constitutive models and statistical analysis of the short-term tensile response of geosynthetics after damage. *Constr. Build. Mater.* **2022**, *317*, 125972. [[CrossRef](#)]
45. Li, X.; Cao, W.; Su, Y. A statistical damage constitutive model for softening behavior of rocks. *Eng. Geol.* **2012**, *143–144*, 1–17. [[CrossRef](#)]

46. Wu, L.Y.; Wang, Z.F.; Ma, D.; Zhang, J.W.; Wu, G.M.; Wen, S.; Zha, M.L.; Wu, L.Z. A continuous damage statistical constitutive model for sandstone and mudstone based on triaxial compression tests. *Rock Mech. Rock Eng.* **2022**, *55*, 4963–4978. [[CrossRef](#)]
47. Deng, J.; Gu, D. On a statistical damage constitutive model for rock materials. *Comput. Geosci.* **2011**, *37*, 122–128. [[CrossRef](#)]
48. Zhou, S.; Xia, C.; Zhao, H.; Mei, S.; Zhou, Y. Statistical damage constitutive model for rocks subjected to cyclic stress and cyclic temperature. *Acta Geophys.* **2017**, *65*, 893–906. [[CrossRef](#)]
49. Sobol, I.M. Sensitivity estimates for nonlinear mathematical models. *Math. Model. Comput. Exp.* **1993**, *1*, 112–118.
50. Saltelli, A. Making best use of model evaluations to compute sensitivity indices. *Comput. Phys. Commun.* **2002**, *145*, 280–297. [[CrossRef](#)]

Disclaimer/Publisher’s Note: The statements, opinions and data contained in all publications are solely those of the individual author(s) and contributor(s) and not of MDPI and/or the editor(s). MDPI and/or the editor(s) disclaim responsibility for any injury to people or property resulting from any ideas, methods, instructions or products referred to in the content.